Data Pre-Processing and Optimization Techniques for Stochastic and Deterministic Low-Order Grey-box Models of Residential Buildings

Xingji Yu[a,*], Laurent Georges[a] and Lars Imsland[b]

[a]Department of Energy and Process Engineering, Faculty of Engineering, NTNU - Norwegian University of Science and Technology, Kolbjørn Hejes vei 1a, 7034 Trondheim, Norway

[b]Department of Engineering Cybernetics, Faculty of Engineering, NTNU - Norwegian University of Science and Technology, O. S. Bragstads plass 2, 7034 Trondheim, Norway

*xingji.yu@ntnu.no

Abstract

Grey-box models are data-driven models where the structure is defined by the physics while the parameters are calibrated using data. Low-order grey-box models of the building envelope are typically used for two main applications. Firstly, they are used as a control model in Model Predictive Control (MPC) where the thermal mass of the building is activated as storage (for instance in demand response). Secondly, they are used to characterize the thermal properties of the building envelope using on-site measurements. The influence of the data pre-treatment on the performance of grey-box models is hardly discussed in the literature. However, in real applications, information about data pre-processing by sensors or data acquisition systems is expected to be limited. Therefore, the influence of the sampling time, low-pass filters and *anti-causal shift* (also called data labeling) are analyzed for grey-box models in deterministic and stochastic innovation form. The influence on the optimizer performance is also investigated. The datasets are generated from virtual experiments using multi-zone building performance simulations of a residential building (in lightweight wooden construction) heated using different types of excitation signals. Results show that the parameters of deterministic grey-box models are significantly influenced by the training data while the data pre-treatment has a limited impact on the model and optimizer performance. Depending on the training data, the value taken by some parameters is not physically plausible. On the contrary, stochastic models are significantly influenced by the data pre-treatment, especially the sampling time, and less by the training data. The parameters can become non-physical for large sampling times. However, the *anti-causal shift* proves to be efficient to keep the parameters almost constant with increasing sampling times. Even though the parameter values of the deterministic model are less physically plausible, the simulation performance of deterministic models is higher than using the equivalent stochastic models. These results suggest that deterministic models seem better suited for MPC while stochastic models are better suited for the characterization of thermal properties (if suitable data pre-treatment is applied).

Keywords: Data pre-processing; Grey-box modelling; Building thermal mass

Nomenclature

DR	Demand Response	*GA*	Genetic Algorithm
MPC	Model Predictive Control	*PSO*	Particle Swarm Optimization
BPS	Building Performance Simulation	*ACS*	Anti-Causal Shift
AMS	Advanced Metering System	*DS*	Direct Sampling
RC	Resistance and Capacitance	*MA*	Moving Average
PRBS	Pseudo-Random Binary Signal	*FIR*	Finite Impulse Response
PI	Proportional Integral	*det*	Deterministic Model
NRMSE	Normalized Root Mean Squared Error	*sto*	Stochastic Model
FHS	Full Heating Season	*HTC*	Heat Transfer Coefficient

1 Introduction

The share of Renewable Energy Sources (RES) is increasing constantly in today's energy system. Power generation from RES is often decentralized and intermittent, such as solar and wind energy, which brings considerable volatility to the electric grid. The supply and demand sides in the power system have to be balanced at each time step. Any power imbalance can cause severe consequences for power quality and reliability (e.g. voltage fluctuations and power outage) [1,2]. Therefore, more flexible loads are needed to further increase the share of intermittent RES. Demand response (DR) is the interaction and responsiveness of the end-use customer to a specific penalty signal (e.g. price signal, CO_2 intensity factor for electricity signal) [3,4]. It is considered to be an important component to provide flexibility for smart grids [5]. In addition, DR can also be used for peak-shaving to avoid congestion [6,7] in the distribution grid so that the reinforcement of these grids can be postponed.

The share of the total final energy consumed by buildings is 20–40% and this is increasing at the rate of 0.5–5% per year in developed countries [8]. In Nordic countries, the building energy consumption is dominated by space-heating due to the long and cold heating season. Building thermal mass can be considered as short-term heat storage and be used to perform DR [9–11], which can contribute to providing flexibility to the smart grid. Model Predictive Control (MPC) is considered a promising technique to apply DR. In an MPC, a dynamic model is used to predict the response of the building to future boundary conditions (e.g. forecast of weather conditions, and production of the energy system). The MPC control agent (computers, built-in intelligent devices, etc.) will take the optimal control decisions based on the predictions of the model and system constraints. In buildings, the constraints for the MPC are usually the power limitation of the SH system, and thermal comfort. The performance of the MPC controller thus strongly relies on the quality of the dynamic model of the system to be controlled. Poor quality models could result in undesired control outcomes (e.g. increased energy cost, violation of thermal comfort, or even be counterproductive for the grid). In practice, MPC is currently applicable for only a small fraction of existing buildings due to cost criteria [12]. However, the ongoing implementation of smart meters, like the Advanced Metering System (AMS) in Norway [13] and "Key principles for the package of ordinances governing smart grids" in Germany [14], will make the MPC control concept more accessible in the future. The recent emergence of small, low-cost and wireless sensors with a data collection function [15] will also contribute to accelerate the implementation of MPC in buildings. Finally, creating a suitable model is acknowledged to be the most time-consuming part of MPC implementation [16]. Therefore, the cost related to the identification of the control model should also be limited to reduce the total investment cost of

the MPC controller. The need to identify a control model at a low cost is even more severe for small residential buildings.

The modelling methods for MPC can be divided into three main categories, namely white-, black- and grey-box models. White-box models are based on physical laws. They require exhaustive information about the building including underlying physical processes, and parameters. This type of model is usually mathematically complex but has high accuracy. This approach is often used in Building Performance Simulation (BPS) software like Modelica [14], EnergyPlus [14] and IDA [17]. However, white-box models are time-consuming to calibrate as a lot of input parameters have to be defined and they need to be updated during the operational lifetime of the building. Moreover, the mathematical complexity requires extensive computational power [9] or the white-box model has to be simplified using linearization and model reduction techniques [18]. All these factors challenge the feasibility of white-box models for the MPC of the existing building. Black-box models are pure data-driven methods based on the measured input and output time-series data from the system. Statistical regression and Artificial Neural Network (ANN) are common mathematical techniques for black-box models [19]. However, this method requires sufficient data for training to guarantee the accuracy of the model [20]. The precision of black-box models is also significantly influenced by data quality. Grey-box modelling is an intermediate strategy between white- and black-box models. It exploits the dominant physical properties of the system to construct the model structure and uses measurement data to estimate the model parameters. Grey-box models have better generalization (extrapolation) properties [21] and usually require less experimental data compared to black-box models [22]. Lumped resistance and capacitance models (i.e. RC models) are a common approach to create grey-box models, which means the thermal conditions of the building are expressed with an electric circuit analogy [23]. Existing work has already applied grey-box models for MPC in buildings. For instance, Coninck et al. [24] made use of a grey-box model identified by monitoring data to implement MPC. Zong et al. [25] used an economic MPC with a multi-zone grey-box model to control the power of heating radiators in a three-story Danish residential house.

This study mainly focuses on the grey-box modelling of the building thermal dynamics. A significant amount of research has already addressed the question of the structure of grey-box models. Viot et al. [26] gave a detailed list of research papers using RC models for the MPC In the study by Fux et al. [27], a one-capacitance model was used to forecast the indoor temperature of a residential building and it gave satisfactory results. Bacher and Madsen [28] used the data collected from an unoccupied office building to identify a suitable model. Models of different orders were evaluated based on likelihood ratio tests. These showed that from third-order, increasing the model order cannot lead to significant improvements in the results. Palomo Del Barrio et al. [29] concluded that a second-order model is sufficient for forecasting results for both indoor temperature and heating power. The study of Reynders et al. [30] also confirmed that the second-order model is enough to deliver decent prediction performance. Moreover, Reynders et al. concluded that heat flux measurements were needed to guarantee observability for higher-order models (i.e. fourth and fifth-order models) since overfitting and convergence problems occurred. Yu et al. [31] compared two grey-box model structures generated from VDI 6007 [32] and ISO 13790 [33]. The results revealed that with limited measurements and a large number of unknown parameters, the parameters of the identified model can easily become non-physical. Brastein et al. [34] showed that deterministic grey-box models at second-order can already face the problem of practical identifiability. Based on these previous findings, our paper only uses first- and second-order grey-box models to address the research questions so that the challenges related to overfitting can be eliminated from the study. When space-heating power is used as input and the indoor temperature is used as an output, previous works showed that second-order models are a good trade-off between accuracy and identifiability. Therefore, our paper only resorts to

first- and (simple) second-order grey-box models to eliminate challenges related to overfitting from the study.

Data pre-processing (or data pre-treatment) is acknowledged to have a key influence on the model identification results [35]. However, this topic has hardly been addressed in the field of grey-box models for buildings. Ljung and Wills [36] revealed several issues when applying a long sampling time to estimate continuous-time models with stochastic disturbances. However, the analysis of Ljung and Wills is illustrated using a theoretical example. Therefore, our paper investigates the influence of long sampling times in building applications. The time-series data is generated using virtual experiments using the BPS software IDA ICE. In addition to the sampling time, the influence of the data pre-processing using a low-pass filter is investigated as well as the influence of shifting the input data in time, called *anti-causal shift* (ACS). In this context, the performance of grey-box models in the deterministic and stochastic innovation forms is compared using the MATLAB identification toolbox [37]. To analyze the model performance, the ability to characterize the thermal properties of the building envelope and the simulation performance are clearly distinguished. The simulation performance is a good indicator of the model accuracy for MPC applications. Finally, these research questions are important as data can be processed (or altered) by sensors, the data acquisition system or by the building modeler prior to the model identification.

The remainder of the paper is structured as follows. Section 2 provides information on the virtual experiment using BPS software, which includes detailed information about the virtual building, the excitation signals and the boundary conditions. Section 3 describes the grey-box model structure used for this study. The model identification tool and method are also outlined, followed by the data pre-processing method. Section 4 shows results split into three aspects. The model performance to characterize the building thermal properties is first discussed. Then, the analysis of the optimizer performance and the simulation performance is analyzed. Section 5 gives some complementary discussions based on the results. Conclusions are presented in Section 6.

2 Virtual experiments

2.1 Detailed multi-zone dynamic simulations

IDA ICE is a detailed dynamic simulation tool to study the indoor environment and the energy consumption of buildings. In this study, an IDA ICE building model is used as a virtual experiment to generate data for system identification. It is a two-story detached house located in Oslo with a heated floor area of 160 m². The building is constructed in wood, meaning a lightweight construction, and complies with the requirement of the Norwegian passive house standard, NS 3700 [38]. The three-dimensional geometry of the building is shown in **Error! Reference source not found.**. The building is equipped with balanced mechanical ventilation with a heat recovery unit. A cascade ventilation strategy is applied. This heat exchanger is modelled using constant effectiveness of 85% without bypass (like a plate heat exchanger) to promote the linearity of the model. This is done because the research focuses on the thermal dynamics of the building envelope and does not aim at modelling the air handling unit (AHU) in detail. Other detailed information regarding the BPS software model can be found in [39].

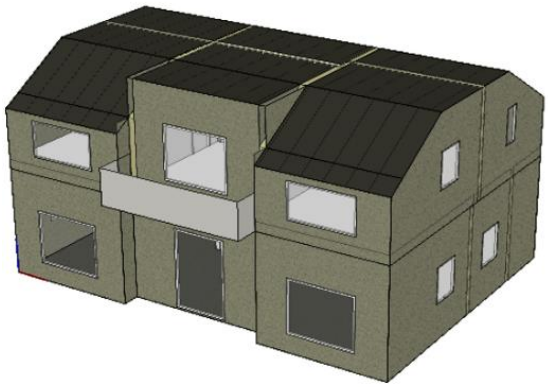

Figure 1: 3D geometry of the building model in IDA ICE (showing the southwest facade).

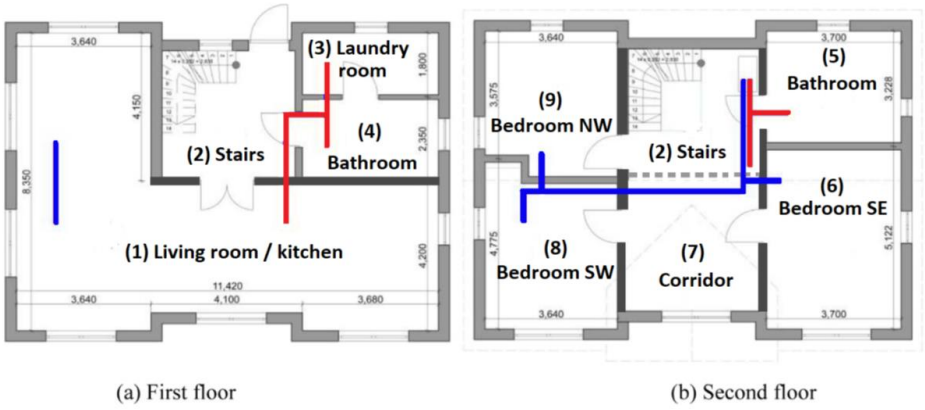

Figure 2: Floor plan of the test building (ducts for the supply air are in blue and in red for extraction).

The detailed building model is multizone and the zoning follows the floor plan presented in Figure 2. For the sake of simplicity, the grey-model models considered in our study are mono zone: it is not necessary to use multi-zone grey-box models to address our research questions. Consequently, the indoor temperature in our virtual experiments should be as uniform as possible. This is done by opening all the internal doors inside the building. IDA ICE has an embedded ventilation network model which accounts for the large bidirectional airflow through open doorways. Thus, the air temperature inside the building computed by IDA ICE is relatively uniform due to the large convective heat transfer between rooms. The volume-averaged temperature is selected to represent the measured indoor air temperature. The mean air temperature of the extract ventilation air is also a common choice. However, based on preliminary investigations, the volume-averaged temperature proved to give better grey-box models for this test case. The building is heated using electric radiators as these are the most common space-heating systems for residential buildings in Norway [40]. This heating system has smaller thermal inertia than the building envelope so that the dynamics of the radiators are expected to play a limited role. Hourly profiles for internal gains generated by artificial lighting, electric appliances and occupancy are taken from the Norwegian technical standard TS3031:2016 [41]. The typical meteorological year (TMY) of Oslo with a resolution of one hour is used for the IDA ICE simulations. Like internal gains, solar gains have thus a resolution of one hour.

2.2 Excitation signals of the building thermal dynamics

The system needs to be perturbed to obtain data for model identification. It is often recommended to use excitations having no correlation with the other inputs [28]. The Pseudo-Random Binary Signal (PRBS) is a periodic and deterministic signal which approximates white noise properties

[42]. The PRBS signal can activate the dynamic system in a large spectrum of frequencies with a high signal-to-noise ratio (SNR) [28,43,44]. In this study, the excitation signal is simultaneously applied to all the electric radiators in the BPS model. Following the guidelines of the IEA EBC Annex 58 [45], the excitation signal is in fact the combination of the two PRBS signals. One sequence to identify the short-time dynamics with a period (T) of 10 minutes and with an order (n) of 8. The second sequence aims at identifying the long time constant of the building with a period (T) of 3.5 hours and n equals to 5. The resulting time profiles for the space-heating are shown in Figure 3. The PRBS signal can be applied to four different weeks in the space-heating season. These weeks are characterized by different weather conditions, as described in Table 1.

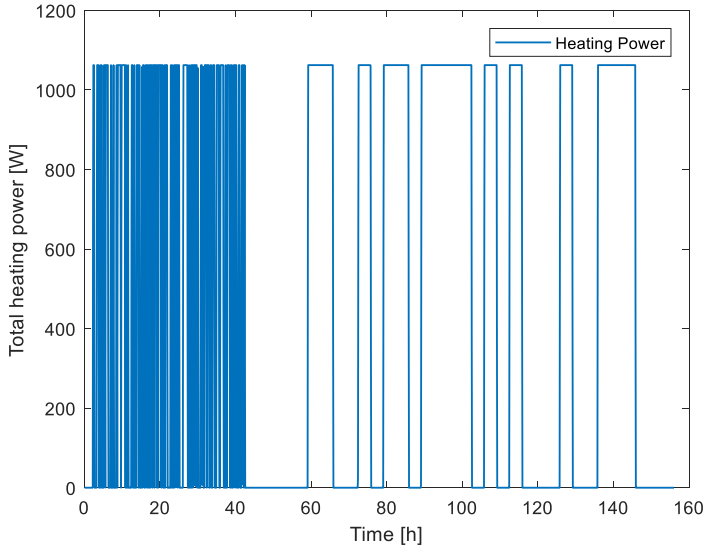

Figure 3: Time profile of the PRBS signal applied to electric radiators.

However, it is not always desirable to apply a PRBS signal to the space-heating system as large variations of the indoor temperature may occur and lead to thermal discomfort for the occupants. Therefore, conventional controls of heating systems are also investigated. Intermittent heating with a temperature setpoint changing between daytime and night-time is considered (i.e. a night setback). Two different local controllers are tested to track the set-point temperature in each room: a Proportional-Integral (PI) control and an on-off control (with a differential of 1K). The last one is the most common control strategy for electric radiators in buildings. When a PRBS signal is applied over a long period of time (i.e. longer than one week), it is difficult to design the signal so that the indoor temperature is kept within comfortable temperature limits for the occupants. By definition, conventional heating controls enable to have normal occupancy of the building during the experiments used to collect data for model identification. It is thus possible to collect data over a longer period of time than one week without impacting the thermal comfort of building users. The full space-heating season (FHS) starting in November and finishing at the end of March can be used to train the model. However, it is also interesting to test whether a shorter training period of one month would be sufficient to train the grey-box models. It is also interesting to check whether specific months are more suited for this task. Therefore, the model parameters are also identified using each of five different months of the space-heating season (i.e. Month 1 to 5).

Table 1: Weather conditions in four PRBS experiments.

Type	Outdoor Temperature	Sky	Date	Duration
Very Cold	-10 °C	Clear sky	12/13/2019	One week

Cold	0 °C	Overcast	12/24/2019	One week
Cold	0 °C	Clear sky	3/23/2019	One week
Mild	5 °C	Overcast	11/23/2019	One week

To investigate the influence of data pre-processing techniques and the grey-box modelling approaches, 20 different datasets have been generated using different excitation signals, duration of the experiment and weather data. The detailed description of each case can be found in Table 2 below. IDA ICE assumes that variables are piecewise linear during one-time step. The model equations are integrated numerically using a variable time-step so that data is not generated at constant time intervals. Consequently, conservative interpolation has been used to interpolate IDA ICE data on a uniform grid of 2.5 min. This time step is significantly smaller than the shortest period of the PRBS (i.e. 10 min).

Table 2: Description of the datasets and their corresponding abbreviation.

Case (dataset)	**Case description (excitation)**	**Period/ Duration**	**Abbreviation**
1	PRBS1	Week 1	W1-PRBS
2	PRBS2	Week 2	W2-PRBS
3	PRBS3	Week 3	W3-PRBS
4	PRBS4	Week 4	W4-PRBS
5	Intermittent on-off	Week 1	W1-Inter I/O
6	Intermittent on-off	Week 2	W2-Inter I/O
7	Intermittent on-off	Week 3	W3-Inter I/O
8	Intermittent on-off	Week 4	W4-Inter I/O
9	Intermittent on-off	Month 1	M1-Inter I/O
10	Intermittent on-off	Month 2	M2-Inter I/O
11	Intermittent on-off	Month 3	M3-Inter I/O
12	Intermittent on-off	Month 4	M4-Inter I/O
13	Intermittent on-off	Month 5	M5-Inter I/O
14	Intermittent on-off	Full heating season	FHS-Inter I/O
15	Intermittent PI	Month 1	M1-PI
16	Intermittent PI	Month 2	M2-PI
17	Intermittent PI	Month 3	M3-PI
18	Intermittent PI	Month 4	M4-PI
19	Intermittent PI	Month 5	M5-PI
20	Intermittent PI	Full heating season	FHS-PI

3 Methodology for grey-box modelling

3.1 Grey-box model structure

Based on the literature review (see the introduction section), only first-order and second-order grey-box models are considered in this paper. Preliminary tests using our virtual experiments confirmed that a third-order model would be overfitted. The structure of the grey-box model expresses the conservation of energy. As mono zone grey-box models are considered (with a single node related to the indoor air temperature), the dominant process to be integrated is the heat transfer between the building and its outdoor environment. The influence of solar radiation

and internal gains are also included in the grey-box models. Two model structures are studied: a one-resistance, one-capacitance (1R1C), and a three-resistance, two-capacitance (3R2C) model. The physical interpretation of their respective parameters can be found in Table 3.

The internal and solar gains can be computed accurately by BPS. For the sake of simplicity, these gains have been introduced directly in the grey-box models rather than identified. For the 3R2C model, only the coefficient α that distributes the solar gains between the two temperature nodes needs to be identified. In real applications, the gains are not known exactly. However, simplifying the problem enables us to emphasize the specific research questions in this paper. To obtain a more physical representation of the heat exchange between the building and its outdoor environment, an equivalent outdoor temperature is applied as described in Harb et al. [9]. This temperature is calculated using Equation 1 with a short-wave absorption coefficient of the exterior surface (a_f) of 0.5 and an exterior heat transfer coefficient (α_A) of 25 W/(m^{2}K):

$$T_{a,eq} = T_a + Q_{irrad} \frac{a_f}{\alpha_A} \qquad (1)$$

Table 3: The physical interpretation of the parameters of the grey-box models.

Parameters	Physical interpretation
T_i	Temperature of interior heat capacity [°C].
T_e	Temperature of the building envelope [°C].
T_a	The outdoor (or ambient) temperature [°C].
$T_{a,eq}$	The equivalent outdoor (or ambient) temperature [°C].
C_i	Heat capacity of the building combining the thermal mass of the air, the furniture, internal walls and, potentially, a fraction of the thermal capacitance of external walls: the first centimeters for the second-order model and a larger fraction for the first-order model [kWh/K].
C_e	Heat capacity of the node external wall for the second-order model [kWh/K].
UA	Overall heat transfer coefficient (HTC) between the building and its ambient, including ventilation [kW/K].
UA_{ie}	Heat conductance between the building envelope and the interior [kW/K].
UA_{ea}	Heat conductance between the ambient and the building envelope [kW/K].
UA_{vent}	Heat conductance between the ambient and the interior node [kW/K].
Q_{int}	Internal heat gain from artificial lighting, people and electric appliances [kW].
Q_{solar}	Heat gain from solar irradiation [kW].
Q_h	Heat gain from the electric heater [kW].
α	Fraction of solar gains to air node.

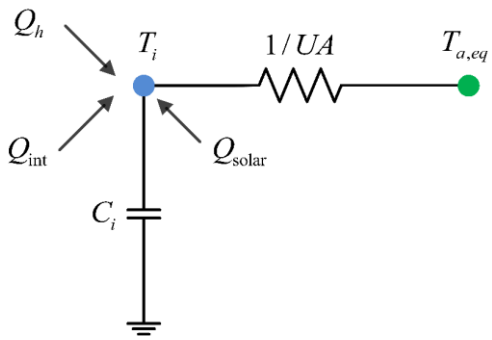

Figure 4: First-order 1R1C model.

The heat dynamics of the 1R1C model is expressed in the following differential equation:

$$C_i \frac{dT_i}{dt} = UA(T_{a,eq} - T_i) + Q_h + Q_{\text{int}} + Q_{solar} \qquad (2)$$

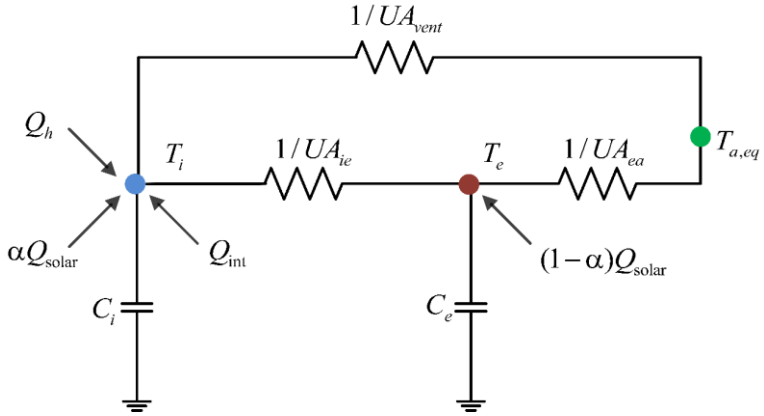

Figure 5: Second-order 3R2C model.

The heat dynamics of the 3R2C model is expressed by the following differential equations:

$$C_i \frac{dT_i}{dt} = UA_{vent}(T_{a,eq} - T_i) + UA_{ie}(T_e - T_i) + Q_h + Q_{\text{int}} + \alpha Q_{solar} \qquad (3)$$

$$C_e \frac{dT_e}{dt} = UA_{ea}(T_{a,eq} - T_e) + UA_{ie}(T_i - T_e) + (1-\alpha) Q_{solar} \qquad (4)$$

3.2 Model identification tool and method

The MATLAB system identification toolbox is used in our study [37]. Madsen et al. [45] illustrated how stochastic models can be formulated as an extension of deterministic models. In the stochastic form, a system noise (or noise term) is added to the deterministic model equations to better account for the modelling approximations, unrecognized inputs and measurement of inputs corrupted by noise. The generic equations of the stochastic linear state-space model in innovation form can be expressed as:

$$\frac{dx}{dt} = Ax(t) + Bu(t) + Ke(t) \qquad (5)$$

$$y(t) = Cx(t) + e(t) \qquad (6)$$

where x is the state vector, A, B and C are the system matrices, u is the input vector (i.e. $T_{a,eq}$, Q_{solar}, Q_{int}, Q_h) and y is the output (i.e. indoor temperature, T_i). K is the disturbance matrix of the

innovation form (Kalman gain) [46]. The matrices A, B, C and K are functions of the model parameters (θ), in our case defined by Equations 2 to 4. The continuous-time model is first discretized so that discrete measurement data can be used to identify the model parameters. Unlike IDA ICE, the time discretization in the MATLAB identification toolbox assumes piecewise-constant input data during each time interval (i.e. zero-order hold). For stochastic models, both the value and variance of the model parameters are identified. In the case of deterministic models, the K matrix is set to zero. The parameter variance is not clearly defined for the deterministic model in the MATLAB system identification toolbox. Therefore, it has been decided to only consider the parameter value.

At the beginning of the identification procedure, the initial guess of the model parameters and their region of feasibility (i.e. lower and upper bounds for each parameter) should be defined by the user as input parameters. Then, the optimizer iterates within the feasibility region to find the value of the parameters that minimize the prediction error criterion $f(x)$

$$f(x) = \sum_{k=1}^{N} \| y_k - \hat{y}_k(\theta) \|^2 \qquad (7)$$

where y_k is the measurement output while $\hat{y}_k(\theta)$ is the one-step ahead prediction.

The default function (*greyest*) in the MATLAB identification toolbox uses gradient-based optimizers. Four different iterative search methods are used in sequence. Consequently, the optimizer may converge to a local optimum if the problem is not convex. As shown in Arendt et al. [47], Genetic Algorithm (GA) combined with a gradient-based method could be used to solve non-convex optimization problems used to identify the parameters of grey-box models. Likewise, a global optimization algorithm has been implemented in our work to avoid a local optimum. A metaheuristic Particle Swarm Optimization (PSO) is applied at the first stage, followed by the default *greyest* function to refine results during the second stage. The PSO algorithm begins by creating the initial particles and assigning them initial velocities. It evaluates the objective function at each particle location and determines the best (lowest) function value and the best location. In the next step, new velocities are chosen based on the current velocity, the particles' individual best locations, and the best locations of their neighbors. The optimizer then iterates the particle locations, velocities, and neighbors until the algorithm reaches a stopping criterion. Detailed information on the PSO algorithm can be found in [48,49]. For each test case, both optimization procedures are used in sequence: the default *greyest* and the global optimization. The method giving the lowest error for the prediction error criterion is selected to provide the model parameters. The flow chart of the identification routine is summarized in Figure 6.

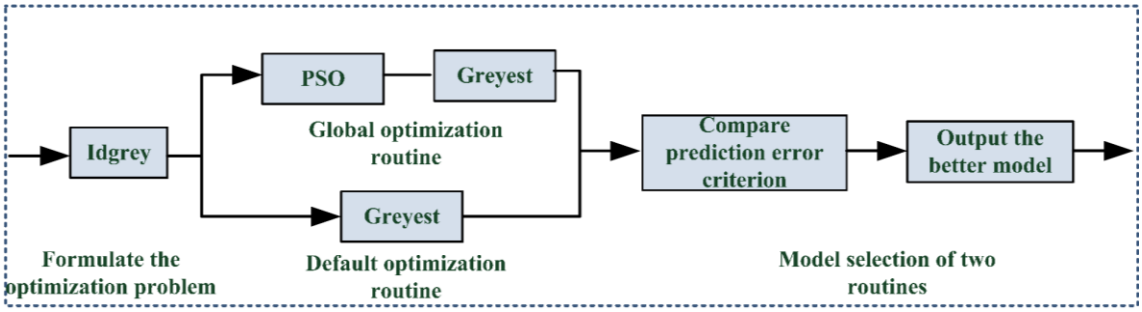

Figure 6: Flow chart of the optimization procedure to identify the model parameters.

3.3 Data pre-processing method

Extended sampling time (T_s) can lead to a non-physical value and variance for the identified parameters of grey-box models (see e.g. [36]). In real-life applications, it can be seldom

guaranteed that measurement data is recorded at a sampling time (T_s) shorter than the shortest time of the system (T_{min}). In our test case, T_{min} is related to the shortest period of the PRBS signal (T) as the other model inputs (namely the internal and solar gains) have a resolution of one hour. T_{min} is therefore 10 min and the sampling time (Ts) applied to the BPS data has been taken at 2.5 min to avoid aliasing. As $T_s < T_{min}$, it is therefore possible to identify the parameters of the grey-box model without facing the above-mentioned issues. However, the measurement data at 2.5 min can be resampled at longer sampling times, namely 15, 30 or 60 minutes, so that the case where $T_s < T_i$ can be directly compared to the cases where $T_s > T_i$. In real applications, it is difficult to guarantee that the data logging is done at a sampling time shorter than the system dynamics. In addition, the measurement data can be pre-processed before being logged at T_s. Two methods are considered here: low-pass filtering and *anti-causal shift*.

Regarding low-pass filtering, three approaches are compared:

- The first approach is direct sampling (DS) at T_s without pre-filtering. This may cause a high aliasing error.
- The second approach applies a moving-average (MA) filter of length T_s before sampling. With MA, the aliasing error is significantly decreased but, in theory, it can still occur.
- The third approach applies a finite impulse response (FIR) filter with a cut-off frequency of $1/T_s$ before sampling. The FIR would lead to negligible aliasing error (if it is designed at a sufficient order).

By analyzing the performance of the three methods, it is possible to understand the influence of aliasing. It is known that these low-pass filters introduce a time delay [35]. However, as the low-pass filters are here applied to all input and output variables of the dataset, the delay does not affect the final identification results. In the paper, we don't distinguish between the low-pass filtering deliberately introduced by the data engineer before training the grey-box model and the low-pass filtering done internally in the sensor. If grey-box models of small residential buildings should be developed at low cost, there is most likely no time to take the technical specifications of each sensor into account. Therefore, the type of data pre-treatment performed by the sensor can be unknown. The analysis is thus generic.

Ljung and Wills [36] pointed out that time labeling plays a role in the alignment of inputs and outputs for the identification application. The results of Ljung and Wills's paper show that a time shift (ACS) of the input (Input Delay = $-T_s$) is beneficial for the model. The method is going to be tested with the data from IDA ICE model.

3.4 Key Performance Indicator

One main application of the grey-box model is MPC. In this context, the long-term prediction performance (i.e. the simulation performance) is paramount. In our work, the NRMSE fitting, defined in Equation 9, is taken as the key performance indicator (KPI) to evaluate the simulation performance. It is based on the normalized root mean squared error (NRMSE) quantifying how well the simulated or predicted model response matches the measurement data, see Equation 8. If the fitting is 100%, this means the model fits the measurement data perfectly, while a low or negative fitting corresponds to a worse model. There are no outliers in the measurement data that will skew the NRMSE KPI, so there is little reason to use KPIs handling outliers better, such as Mean Absolute Error (MAE).

$$NRMSE = \frac{\| y_k - \hat{y}_k \|}{\| y_k - mean(y_k) \|} \qquad (8)$$

$$NRMSE_{fit} = (1 - NRMSE) \times 100\% \qquad (9)$$

Regarding the characterization of the building thermal properties, the performance of the grey-box is evaluated using the physical plausibility of the identified parameters. The calibrated value of the model parameters should give a physically-reasonable estimate of the thermal building properties.

- The overall heat transfer coefficient (HTC) is the total heat loss of the building in a steady-state. Convective and long-wave radiative heat transfer are non-linear. However, in the case of a highly insulated building, the heat conduction is dominant and often assumed linear in BPS (like in IDA ICE). In addition, the heat recovery effectiveness is constant, making its model linear. Specifically, each resistance R (or conductance) of the grey-box model will be dependent on the excitation signal. However, their combination to form the HTC is a steady-state performance parameter. Consequently, the HTC does not depend much on the excitation signal used for the identification. For the first-order model, the HTC is equal to the conductance UA. For the second-order model, the formula of the HTC for the 3R2C model is defined by Equation 10. In conclusion, to be physically plausible, the identified HTC should be close to steady-state heat losses of the IDA ICE model. These losses have been evaluated at 85 W/K (identified by applying a step function of the space-heating to the IDA ICE model).

$$HTC = \frac{1}{1/UA_{ie} + 1/UA_{ea}} + UA_{vent} \qquad (10)$$

- The capacitances (C_i and C_e) are strongly related to the building thermal dynamics. Defining their physical plausibility is more challenging because their value depends on the excitation signal. The effective heat capacitance of the building (C_{eff}) based on the ISO 13786:2017 [50] is taken as a reference value for the capacitances mostly related to the walls (meaning C_i in the 1R1C model and C_e in the 3R2C models). C_{eff} is evaluated assuming daily fluctuations (i.e. 24 hours) and using the thermal properties of each layer in the building walls (i.e. physical-based approach). C_{eff} is here equal to 3.9 kWh/K. To be physically plausible, it is expected that the identified values, also considering their variance, have the same order of magnitude as C_{eff}. Indeed, none of the excitation signals used in our investigations have fluctuations significantly longer than one day. For the 3R2C model, there is no point of comparison for the identified value of C_i. However, as it is related to the fast dynamics of the building, it is expected to be smaller than C_{eff}. In addition, the value of C_i should decrease with increasing frequencies in the excitation signal.

4 Results

In this section, the model performance to characterize the building thermal properties is first discussed, followed by the analysis of the optimizer performance. Finally, the simulation performance, important for MPC applications, is investigated. The comparisons of this section are mainly based on the performance criteria defined in the previous section. However, there are 20 different training datasets (see Table 2), four different models, four different sampling times, two different optimizers and three pre-filtering methods of the virtual experiments, with and without a causal shift. It corresponds to a total of 4320 different test cases. Thus, only the most representative test cases are taken to illustrate the results and support the conclusions.

4.1 Characterization of the building thermal properties

The physical plausibility of the identified grey-box model parameters is verified. It means the ability to identify values for the parameters that are in line with physics. For the sake of the

conciseness, we mainly focus on datasets 1 to 4 with a short training period but strong excitation as well as dataset 14 which has the largest amount of data, see Table 2. These datasets can be seen as extreme scenarios so that it makes them representative to illustrate the model performance. Other datasets are also occasionally used to better illustrate how the input data influences the identification results. As has been mentioned previously in Section 3.3, it has been demonstrated theoretically that ACS of the input signal can be beneficial for model identification[36]. Therefore, the influence of the ACS is tested. The 3R2C model is used to illustrate the results. Some of the results of the 1R1C model are given in Appendix A. Regarding the physical plausibility of parameters, the overall heat transfer coefficient (HTC) of the building and heat capacitances (C_e and C_i) are used to illustrate the results.

All the figures in this section are based on the same layout, see e.g. Figure 7. In each figure, five cases or datasets are considered. The abbreviation for each case on the horizontal axis follows the description given in Table 2. The influence of increasing sampling times on these five cases is reported from the left to the right of the figure. Each figure also distinguishes the cases as a function of the data pre-treatment. Firstly, the colors of markers correspond to the different pre-filtering techniques. The cases in red, blue and black represent the MA filter, the FIR filter and the direct sampling, respectively. Secondly, cases without ACS are shown by circles in normal colors while cases with ACS are shown by triangles in lighter colors.

4.1.1 Deterministic 3R2C model

In Figure 7, the value of HTC is close to the reference value of 85 W/K. The same conclusion is obtained for the 1R1C deterministic model, see Figure 18 in Appendix A. The sampling time (T_s) does not have a noticeable influence on the HTC. Likewise, the pre-filtering method and ACS have no significant impact on HTC.

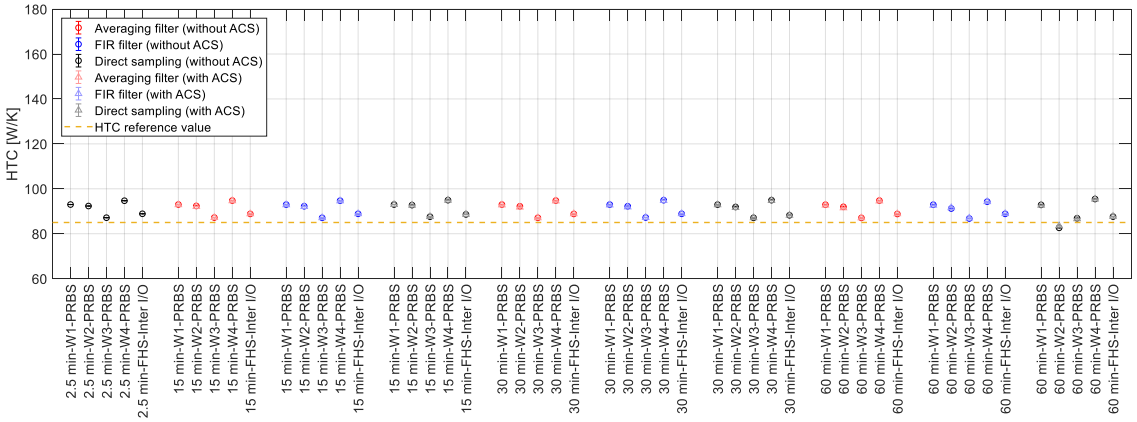

Figure 7: Identified HTC of the 3R2C deterministic model for the cases 1,2,3,4 and 14, different sampling times and pre-filtering techniques; cases with ACS are shown by triangles in lighter colors.

As shown in Figure 8, the training dataset has the largest influence on C_e while the sampling time, the pre-filtering technique and the ACS have a limited impact. The value of C_e is similar between the four datasets using PRBS excitation (i.e. cases 1 to 4) and is plausible compared to the C_{eff} of 3.9 kWh/K determined using standards. However, it differs for case 14 that generates a higher value, well above 3.9 kWh/K. Comparable results are observed for the 1R1C deterministic model (see Figure 19Figure 19 in Appendix A). To further illustrate the influence of the dataset, the values of C_e identified using an intermittent on-off excitation during each month of the space-heating season are compared, i.e. cases 9 to 13, in Figure 9. Even though the excitation signal is generated from the same control (i.e. intermittent on-off control) and has the same duration of one month, the identified C_e strongly depends on the selected period used to train the model,

meaning the specific month of the space-heating season.

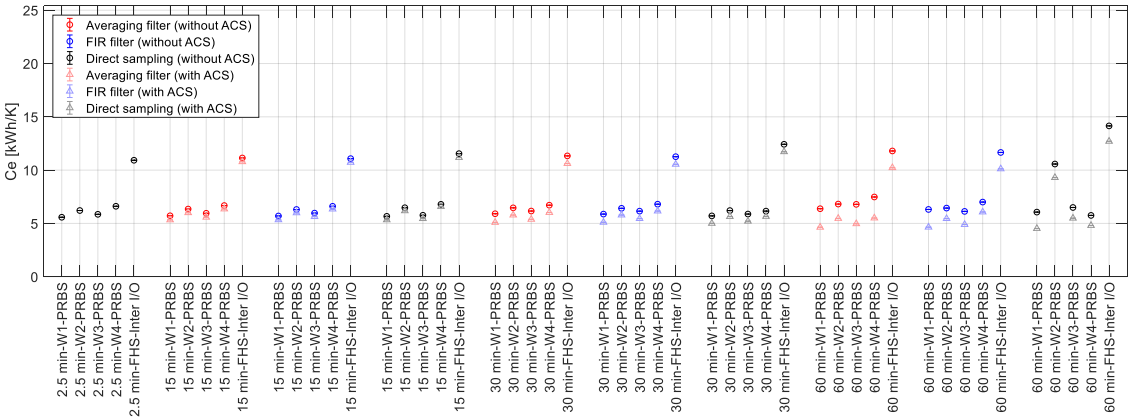

Figure 8: Identified C_e of the 3R2C deterministic model for the cases 1,2,3,4 and 14, different sampling times and pre-filtering techniques; cases with ACS are shown by triangles in lighter colors.

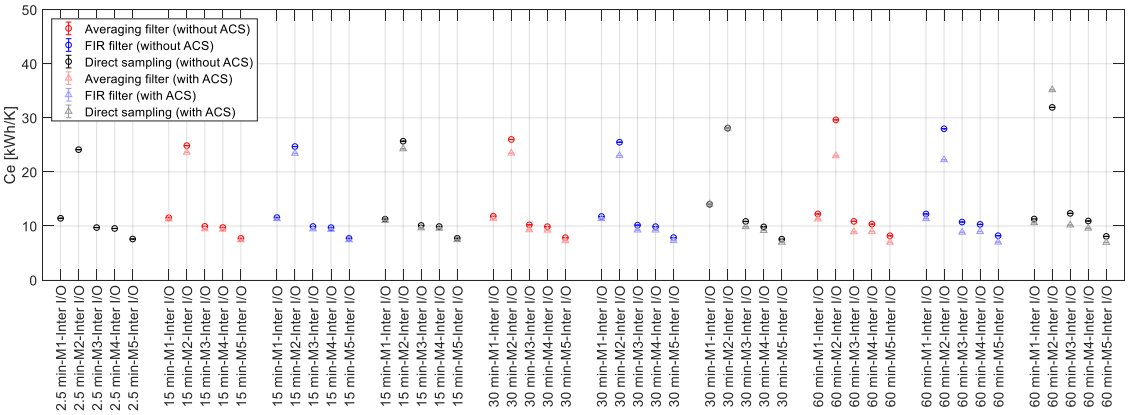

Figure 9: Identified C_e of the 3R2C deterministic model for cases 9 to 13, different sampling times and pre-filtering techniques; cases with ACS are shown by triangles in lighter colors.

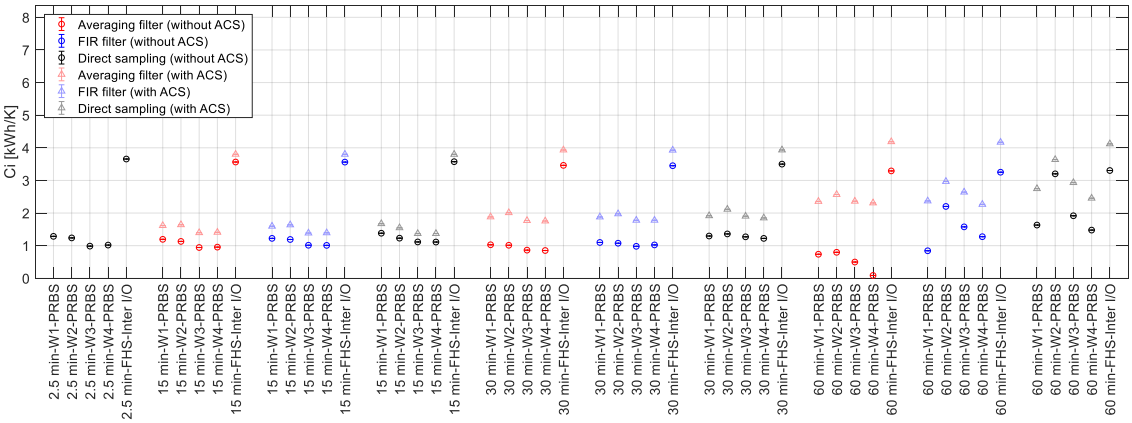

Figure 10: Identified C_i of the 3R2C deterministic model for the cases 1,2,3,4 and 14, different sampling times and pre-filtering techniques; cases with ACS are shown by triangles in lighter colors.

As shown in Figure 10, similar results are obtained for the values of C_i. The case with ACS shows a progressive increase of C_i with the sampling time. A possible reason is that C_i represents the thermal capacitance of the building combining the air, the furniture, internal walls and, potentially, the first centimeters of external walls. With increasing T_s, the high frequencies of the inputs and the output are reduced while the low frequencies, corresponding to a longer penetration

depth in the walls, have more importance in the evaluation of the thermal capacitance. With longer penetration depths, more thermal mass is activated leading to a higher C_i.

Several conclusions can be drawn. Firstly, the value of the parameters strongly depends on the dataset selected to train the model. Both the type of excitation (e.g. PRBS and on-off intermittent excitation) and the selected period during the space-heating season influence results. Secondly, the pre-processing of data does not have a large influence. Neither the ACS, the pre-filtering technique nor the sampling time leads to a significant change in the parameter values. The only exception appears with very large T_s. Then, the pre-filtering can prevent the parameter value from becoming non-physical. Finally, the HTC characterizing the steady-state performance of the building has rather stable values while the other parameters characterizing the thermal dynamics of the building, here C_e and C_i, are more strongly impacted by the training dataset and the sampling time.

4.1.2 Stochastic 3R2C model

For stochastic models, the value and variance of the model parameters are available. However, as the HTC is the combination of the three conductances in the 3R2C model, only the value of the HTC can be shown, not its variance. The value for HTC for the 3R2C stochastic model in Figure 11 is similar to the deterministic model in Figure 7. The same conclusion can be made for the 1R1C stochastic model, shown in Figure 20 in Appendix A. As for the deterministic model, long sampling time can lead to a non-physical value of the HTC. While all the pre-filtering prevented the value to become non-physical for the deterministic model, only the moving-average filter and the ACS have the same effect for the stochastic model.

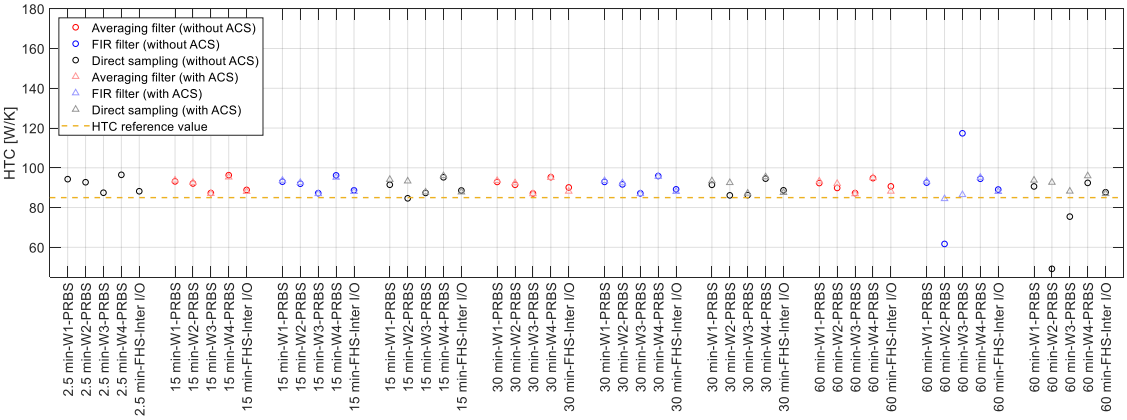

Figure 11: Identified HTC of the 3R2C stochastic model for the cases 1,2,3,4 and 14, different sampling times and pre-filtering techniques; cases with ACS are shown by triangles in lighter colors.

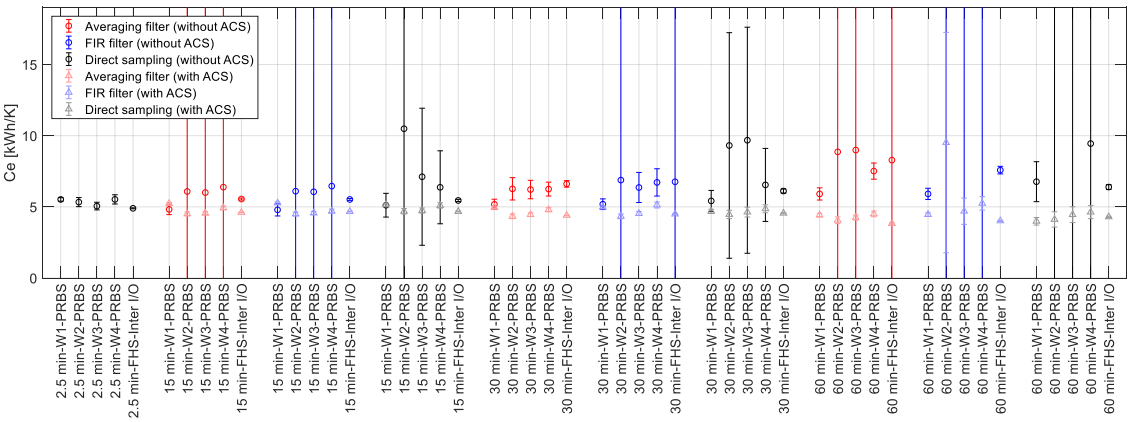

Figure 12: Identified C_e of the 3R2C stochastic model for the cases 1,2,3,4 and 14, different sampling times and pre-filtering techniques; cases with ACS are shown by triangles in lighter colors.

The value and variance of C_e are shown in Figure 12. As long as the sampling time is shorter than the system dynamics (i.e. T_s equal 2.5 min), the value of C_e is independent of the training period and its variance is limited. Close to the C_{eff} of 3.9 kWh/K, the value of C_e is meaningful from a physical point of view. When the sampling time increases, the behavior should be distinguished with and without the application of an ACS. When the ACS is applied, the value and variance of C_e are regular even with long sampling time. The ACS has a strong positive effect on the physical plausibility of C_e. With ACS, pre-filtering has a limited influence on the results. Without ACS, the parameter value and variance become erratic with increasing T_s. Some values are so high that they fall outside the y-axis limit of the graph. In addition, no clear trend can be found on the influence of the pre-filtering and training period.

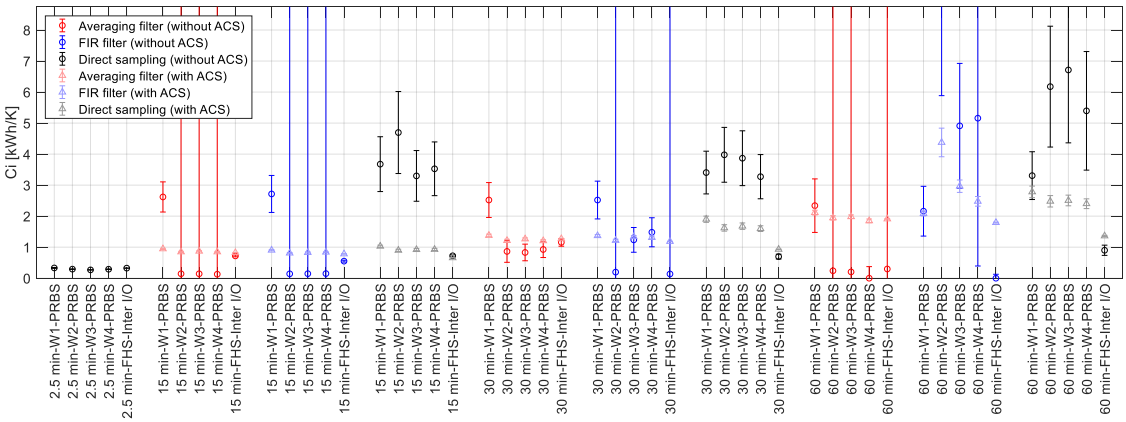

Figure 13: Identified C_i of the 3R2C stochastic model for the cases 1,2,3,4 and 14, different sampling times and pre-filtering techniques; cases with ACS are shown by triangles in lighter colors.

The same phenomenon is observed for the value and variance of C_i in Figure 13. Nonetheless, there is one aspect that differs from C_e. As for the deterministic model with ACS, the values of C_i with the corresponding stochastic version also tends to increase with the sampling time. A possible explanation for this phenomenon has been given in the previous subsection.

From all the results of the stochastic models, several conclusions can also be drawn. First, the identified parameters are strongly dependent on the sampling time. The identified parameters are always consistent if the T_s is taken small compared to the shortest time of the system T_{min} (influenced by the excitation). It is only when T_s gets equivalent or larger than the building dynamics that the parameters are getting non-physical without ACS, especially the thermal capacitances. The second conclusion is that ACS prevents the parameter value and variance to get non-physical for large T_s. With ACS, the uncertainty of the parameters remains limited and their value remains physically plausible. Also with ACS, the values identified are mainly based on the training dataset but to a much smaller extent than the deterministic model. Pre-filtering only has limited influence with ACS while the pre-filtering influence without ACS does not show a clear trend, sometimes improving or degrading results. Finally, like the deterministic model, the steady-state characteristics HTC is less influenced by the dataset and pre-processing than the thermal capacitances.

4.2 Performance of the optimizer

The performance of both optimizers defined in Section 3.2 is compared for a selected number of datasets (i.e. cases 1 to 4 and 14), with and without ACS, for both deterministic and stochastic models. **Error! Not a valid bookmark self-reference.** shows the optimizer that leads to the

lowest prediction error for each test case. The symbol "D" represents the default *greyest* function, "G" represents the two-stage global optimization algorithm and the symbol "≈" is used when both optimizers lead to extremely close results in terms of prediction error and estimation of the model parameters. Only results for the sampling times of 2.5 and 30 min are presented in **Error! Not a valid bookmark self-reference.**. However, the same conclusions are found for the other two sampling times (i.e. 15 and 60 minutes).

Table 4: Optimizer leading to the lowest prediction error: each cell of the table has two symbols, one for the case without ACS (left) and the other with ACS (right); the symbol "D" means default greyest, "G" means global optimization and "≈" means equal performance.

Time (Ts)	Case	1R1C *DS* *(det)*	1R1C MA *(det)*	1R1C *FIR* *(det)*	3R2C *DS* *(det)*	3R2C MA *(det)*	3R2C *FIR* *(det)*	1R1C *DS* *(sto)*	1R1C MA *(sto)*	1R1C *FIR* *(sto)*	3R2C *DS* *(sto)*	3R2C MA *(sto)*	3R2C MA *(sto)*
2.5min	**1**	≈/≈	-	-	≈/≈	-	-	G/≈	-	-	G/≈	-	-
	2	≈/≈	-	-	≈/≈	-	-	G/≈	-	-	G/≈	-	-
	3	≈/≈	-	-	≈/≈	-	-	G/≈	-	-	G/≈	-	-
	4	≈/≈	-	-	≈/≈	-	-	G/≈	-	-	G/≈	-	-
	14	≈/≈	-	-	≈/≈	-	-	G/≈	-	-	G/≈	-	-
30min	**1**	≈/≈	≈/≈	≈/≈	≈/≈	≈/≈	≈/≈	G/≈	G/≈	G/≈	G/≈	G/≈	G/≈
	2	≈/≈	≈/≈	≈/≈	≈/≈	≈/≈	≈/≈	G/≈	G/≈	G/≈	G/≈	G/≈	G/≈
	3	≈/≈	≈/≈	≈/≈	≈/≈	≈/≈	≈/≈	G/≈	G/≈	G/≈	G/≈	G/≈	G/≈
	4	≈/≈	≈/≈	≈/≈	≈/≈	≈/≈	≈/≈	G/≈	G/≈	G/≈	G/≈	G/≈	G/≈
	14	≈/≈	≈/≈	≈/≈	≈/≈	≈/≈	≈/≈	G/≈	G/≈	G/≈	G/≈	G/≈	G/≈

It is observed that the two optimizers have identical results for all the cases using a deterministic model, regardless an ACS is applied or not. However, global optimization generally performs better than the default *greyest* optimization for stochastic models without ACS. On the contrary, both optimizers have similar performance when ACS is applied. It means that ACS tends to preserve the physical plausibility of the model parameters when T_s is large but it also positively influences the convexity of the optimization problem. In general, results confirm that it is better to use global optimization. Otherwise, the obtained sets of parameters are possibly located at a local minimum which mainly depends on the initial guess of the parameters.

4.3 Simulation performance of the models

The simulation performance of the grey-box models, analyzed here using the NRMSE fitting, is another important aspect of the system identification. As expected, the second-order 3R2C model has better simulation performance than the first-order model and is used to illustrate the results. Again, only a limited set of results can be shown. The simulation performance of the 3R2C model trained on the FHS intermittent on-off dataset (i.e. case 14) is taken. This training period covers the whole space-heating season and leads to the lowest variance of the identified parameters in Section 4.1. Then, the simulation performance of the model trained on the case 14 is evaluated on cases 1 to 4, as cross-validation test cases. In simulation, the full length of each dataset is taken as the prediction horizon for both the deterministic and stochastic models. Figure 14 and Figure

15 illustrate the influence of the number of steps ahead on the NRMSE fitting for the 3R2C stochastic model and datasets 1 and 2. The NRMSE fitting for long k-step ahead prediction (i.e. more than two days) is slightly higher than that in a simulation. To study the influence of the data pretreatment, the 3R2C is trained on case 14 with different sampling times as well as with and without pre-filtering.

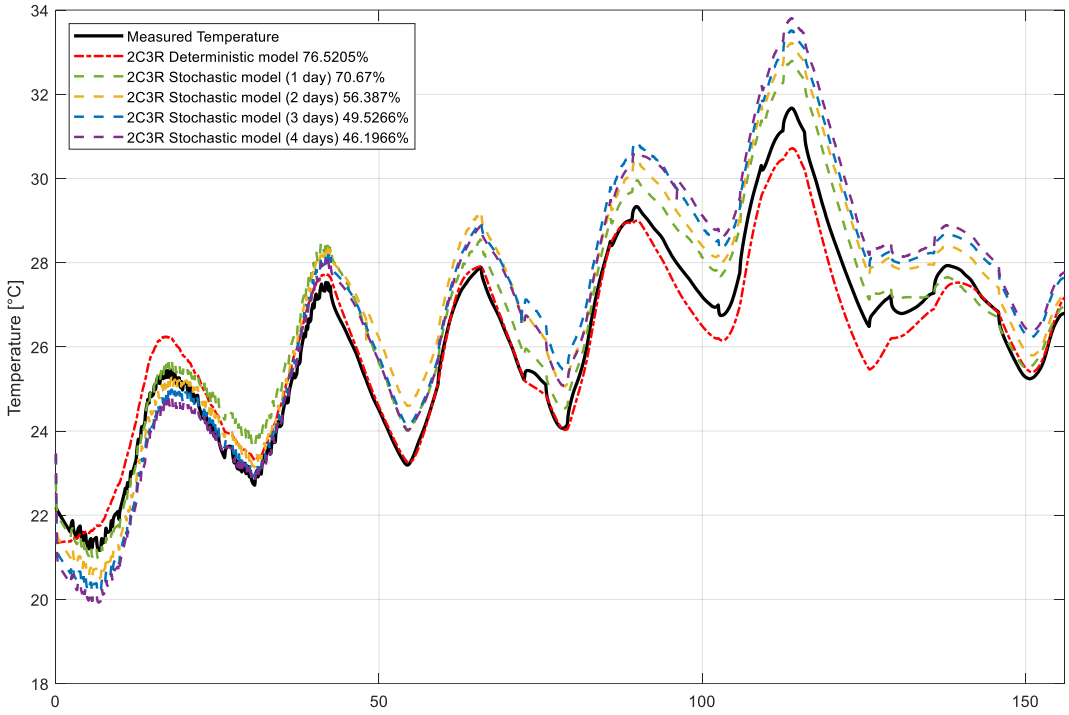

Figure 14: Simulation performance of the deterministic and stochastic 3R2C models with different simulation length for the stochastic model, trained with the dataset 14 and validated with dataset 1.

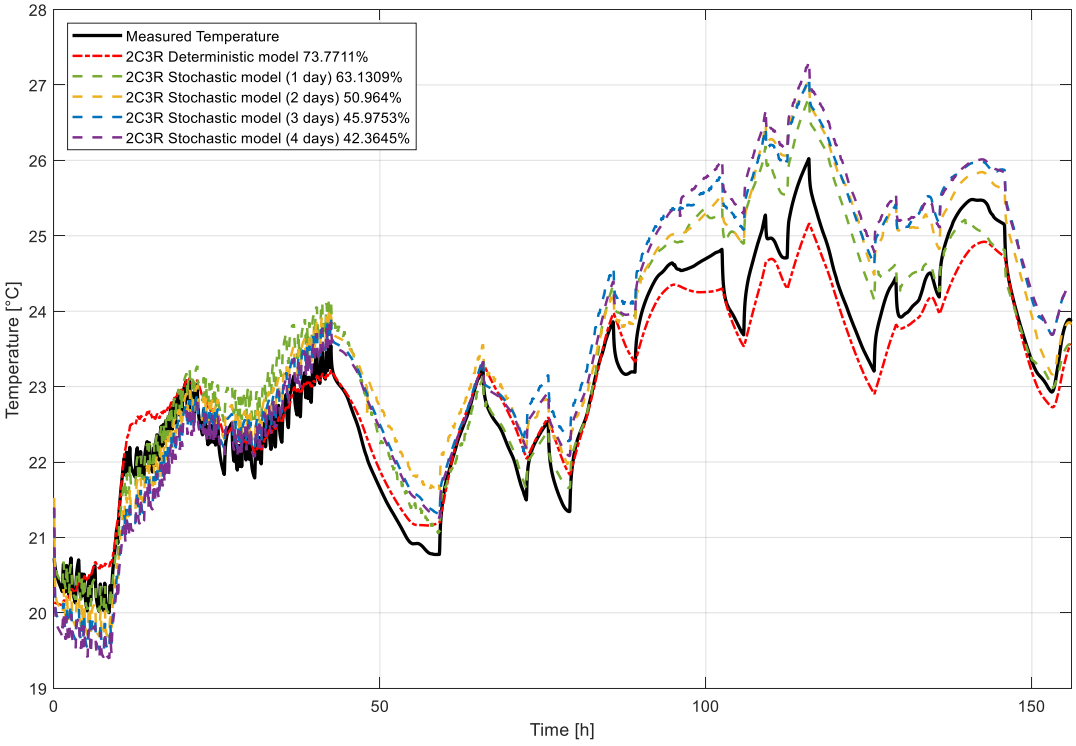

Figure 15: Simulation performance of the deterministic and stochastic 3R2C models with different simulation length for the stochastic model, trained with the dataset 14 and validated with dataset 2.

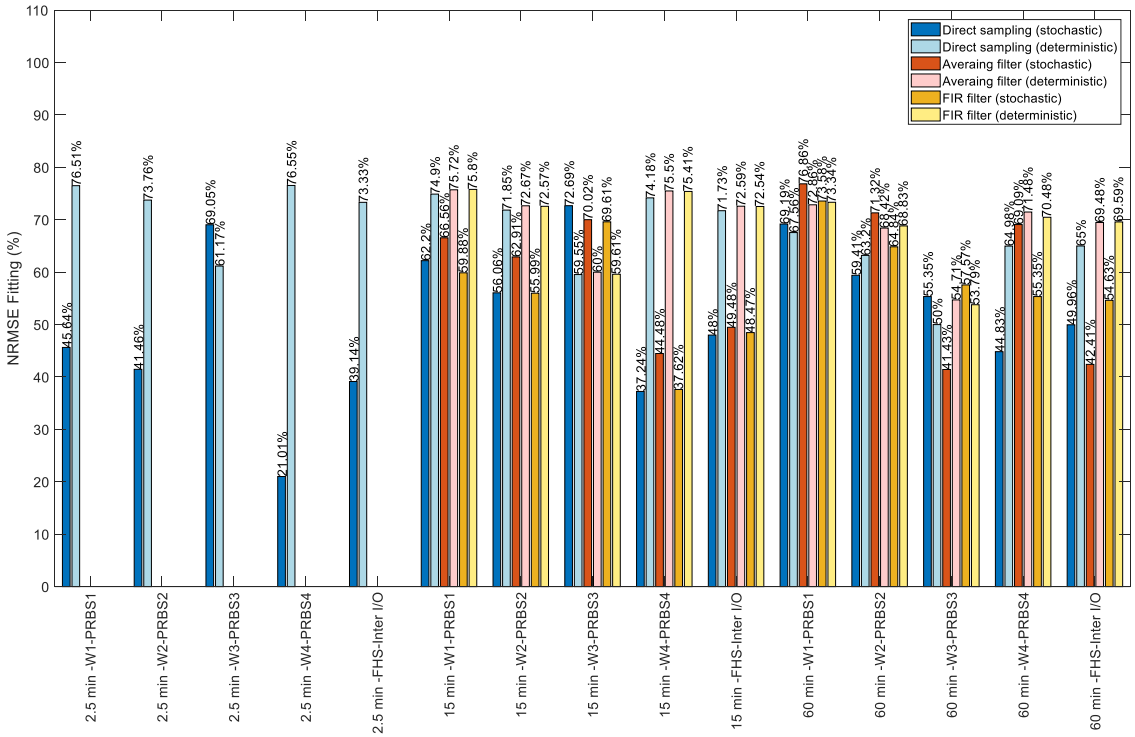

Figure 16: Comparison of the simulation performance of the deterministic and stochastic 3R2C models trained on the dataset 14 without ACS and validated using the other datasets.

Figure 16 compares the simulation performance of the deterministic and stochastic models without ACS. For different T_s and pre-filtering approaches, the deterministic model has a more constant simulation performance than the corresponding stochastic model. For the deterministic model, the NRMSE fitting tends to slightly decrease with increasing T_s while it tends to increase for the stochastic models (except for the PRBS3 case). The deterministic model has generally a better simulation performance than its corresponding model in stochastic form even though this difference tends to disappear for large T_s. This conclusion is noteworthy as for deterministic models the value of the parameters is significantly influenced by the training period and some of the values are even not physically plausible. In other words, identifying a model with parameters that have a more physical value does not necessarily lead to a model with better simulation performance. If one is not interested in the characterization of the thermal properties but rather the simulation performance (like in MPC), results suggest that deterministic models can be more robust than stochastic models. This makes the resolution of the optimization problem to calibrate the model easier (as both local and global optimizer lead to the same parameters). In addition, it has been shown that pre-filtering techniques and T_s have a limited effect on model performance. This conclusion is important in the context of the design of MPC for small residential buildings where a control model should be identified at a low cost, potentially using a fully automated procedure.

Figure 17 compares the simulation performance of the stochastic model with and without ACS. While the ACS tends to improve the physical plausibility of the model parameters and positively influence the optimization problem, it has in general a negative influence on the simulation performance of the model. As already mentioned, the NMRSE fitting generally increases with T_s for the stochastic models without ACS. This increase is less pronounced for the stochastic model with ACS even though the physical plausibility of the parameters has been improved. Two conclusions can be given. Firstly, it confirms that parameters that are more physically plausible

do not necessarily lead to better simulation performance. Here, with large T_s and without ACS, the value of some parameters, such as C_e in Figure 12, is non-physical but it nonetheless leads to better simulation performance. Secondly, the ACS showed to be a robust solution to characterize the thermal properties of the building and the resolution of the optimization problem. However, it appears from our investigations that the ACS comes at the price of lower simulation performance. Finally, none of the approaches investigated here manages to combine high physical plausibility and the highest simulation performance at large T_s.

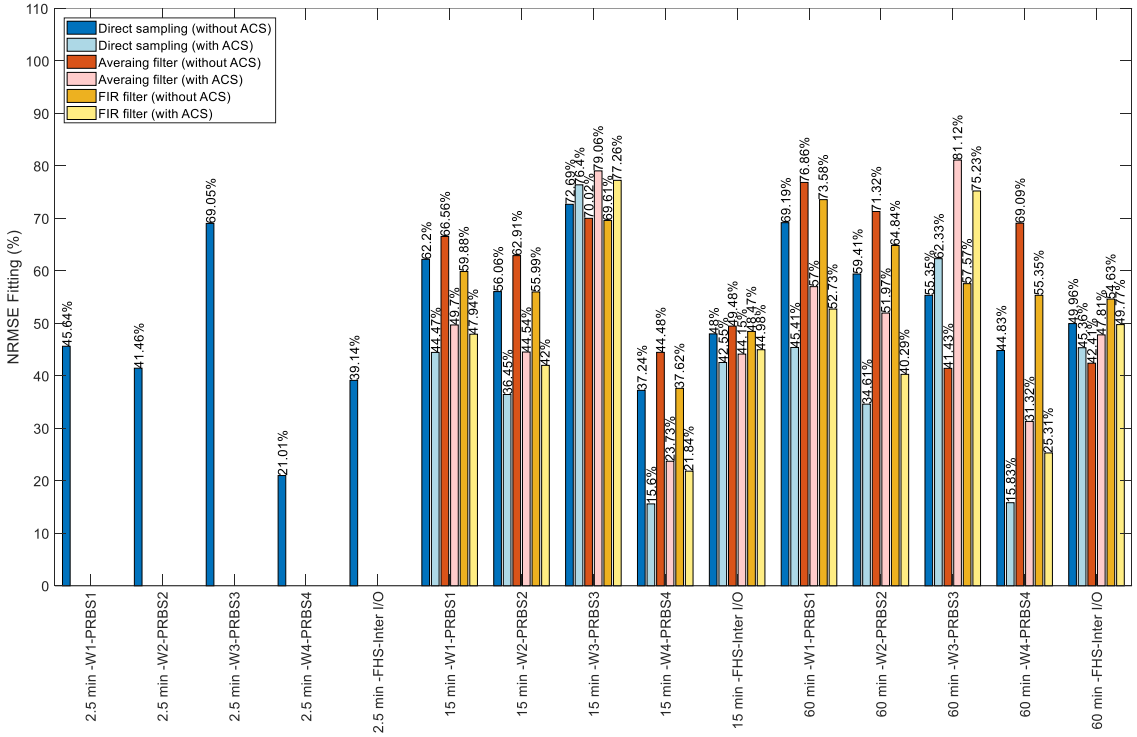

Figure 17: Comparison of the simulation performance of the stochastic 3R2C model with and without ACS, trained with the dataset 14 and validated with datasets 1 to 4.

5 Discussions

Based on the analysis of the results, some complementary discussions can be given:

- Even though ACS has a beneficial effect on the performance of the stochastic grey-box model, the fundamental reason for explaining this phenomenon is not given in the paper. From the authors' knowledge, no clear explanation has been given in the literature as well.
- The simulation performance is a good indicator of modeling accuracy in MPC applications. In Figure 14, it can be seen that the k-step ahead prediction of two days (or more) has a NRMSE fitting close to simulation mode. It shows that the simulation performance is a good indicator even though the prediction horizon used in MPC is well shorter than the entire simulation period. However, even though it is a good indication, it is no mathematical proof that a model with higher simulation performance would systematically outperform another model with lower simulation performance when implemented in an MPC. It should be tested using an MPC test case and conclusions will most probably depend on the MPC test case selected.
- The results and conclusions of this paper are based on the stochastic grey-box model in innovation form. It is not proven that the results can be directly extrapolated to all

formulations of the stochastic differential equations (for instance, the statistical grey-box modelling toolbox of CTSM-R [28]).

- The results and conclusions of this paper are based on the first- and second-order models. It is not guaranteed that the results can be extrapolated to a higher order. For instance, previous investigations have shown that overfitting may occur in third-order models which may lead to more complex analysis. In addition, the exact solar and internal gains have been applied to the grey-box models (i.e. they have not been identified). Furthermore, except for the solar gains, the distribution of the internal gains and the space-heating power between the two nodes of the 3R2C model has been fixed, based on the literature. If all these fixed parameters had also to be identified, it would have significantly increased the number of degrees of freedom and overfitting may have already appeared at second order [34].
- In real applications, the measurements would have some noise due to the sensor precision or the resolution of the data loggers. For some additional test cases not reported in the paper, artificial noise has been added to the IDA ICE measurements. For these cases, this artificial noise did not lead to changes in the conclusions. However, there are many different ways to define this measurement noise. For future work, a sensitivity analysis of the measurement noise should thus be performed in more systematic way to better understand how it affects the conclusions of this paper. Even though our study does not have measurement noise, it does have process noise. For instance, the IDA ICE model is multi-zone with a complex non-linear convective heat transfer between zones while the grey-box model is only mono-zone. Finally, in real applications, the air temperature measurements can be impacted by complex heat flows such as the building fabric, solar irradiation, low ventilation in the thermostat casing or occupant behavior. Such influences on the conclusions should also be analyzed in future work.
- The data series in this paper are based on virtual experiments using detailed dynamic simulations of one test case. As future work, it would be interesting to generalize results to other test cases and also using field measurements in real buildings.

6 Conclusions

The main objective of this paper is to investigate the influence of data pre-processing techniques and optimization approaches on the performance of grey-box models. Both the deterministic model and stochastic grey-box model in innovation form are investigated using the MATLAB system identification toolbox. The analysis is limited to first- and second-order grey-box models. Different excitation signals have been considered to generate input-output data. Three main aspects of grey-box models have been investigated: (1) the physical plausibility of the identified model parameters, (2) the performance of gradient-based compared to global optimizers and (3) the simulation performance. Among pre-processing techniques, the influence of the data pre-filtering (using an MA or an FIR), the sampling time (T_s) and the application of *anti-causal shift* (ACS) have been investigated. In general, it is shown that pre-filtering only has a limited influence so this is not discussed in detail in the conclusions. The conclusions appear to be distinct for the deterministic and stochastic models. Regarding the excitation signal, results also showed that the intermittent heating with on-off control of the electric radiators is a good excitation signal. It enables normal occupancy of the building and the collection of long data series as well as contain both slow daily and fast dynamics.

Regarding the physical plausibility of parameters:

- For deterministic models, the data pre-processing has a limited influence on the identified results. The identified parameters are strongly dependent on the types of excitation and the

training period. The value taken by some of the parameters, especially the thermal capacitance, is not always physically plausible (even for the first-order model).

- For stochastic models, the identified parameters are physical if the sampling time (T_s) is much smaller than the higher frequency of the system to be identified.
- For large T_s and stochastic models, the parameters become non-physical without ACS (even for the first-order model). ACS is extremely beneficial to guarantee the physical plausibility of parameters, making the identified parameters not sensitive to the sampling time anymore.

Regarding the performance of the optimizer:

- For the deterministic and stochastic models, the sampling time (T_s) does not influence the optimizer performance.
- For the deterministic model, the identification results from the default gradient-based and global optimization routines are almost identical (with and without ACS). It seems non-convexity does not play a prominent role in this case.
- For the stochastic model, noticeable non-convexity effects already emerged from the first-order grey-box model (if ACS is not used). The two-stage global optimization leads to lower NRMSE than the default gradient-based optimizer and the resulting parameters have significantly different values. The non-convexity effects disappear if ACS is applied.

Regarding the simulation performance and the model application:

- The deterministic model has in general a higher simulation performance compared to the corresponding stochastic model. In our investigation, this difference tends to disappear for long sampling times. If one is not interested in the characterization of the thermal properties of the building but rather the simulation performance (important for MPC), results show that deterministic models can be a robust strategy as the simulation performance is not influenced much by the sampling time and the pre-filtering. In addition, the optimization problem appears more convex than the corresponding stochastic model. All these aspects can be valuable for the development of inexpensive control models for MPC applications where the identification procedure needs to be (partly) automated and where the information on the measurement accuracy and data acquisition system is limited. Finally, if the only focus is on simulation performance, it is worth questioning whether a grey-box model with parameters that have limited physical meaning have any added value compared to a black-box model. Therefore, in future work, it would be worth comparing the simulation performance of grey-box and black-box models.
- The ideal situation would be to combine physical plausibility with the highest simulation performance. Using stochastic models, a robust evaluation of the thermal properties requires the application of ACS which tends to reduce the simulation performance of the stochastic model. In this study, stochastic models appear more suitable for the characterization of the thermal performance of the building and results suggest this can be difficult to combine with the best simulation performance. However, it remains to be investigated whether the simulation performance of the stochastic model with ACS leads to acceptable accuracy when applied to an MPC.

Acknowledgments

This work is conducted in the framework of the Norwegian Research Centre on Zero Emission Neighbourhoods in Smart Cities (ZEN), co-funded by Research Council of Norway and industry partners. In addition, Ning Guo has helped to review and edit the manuscript.

Appendix A

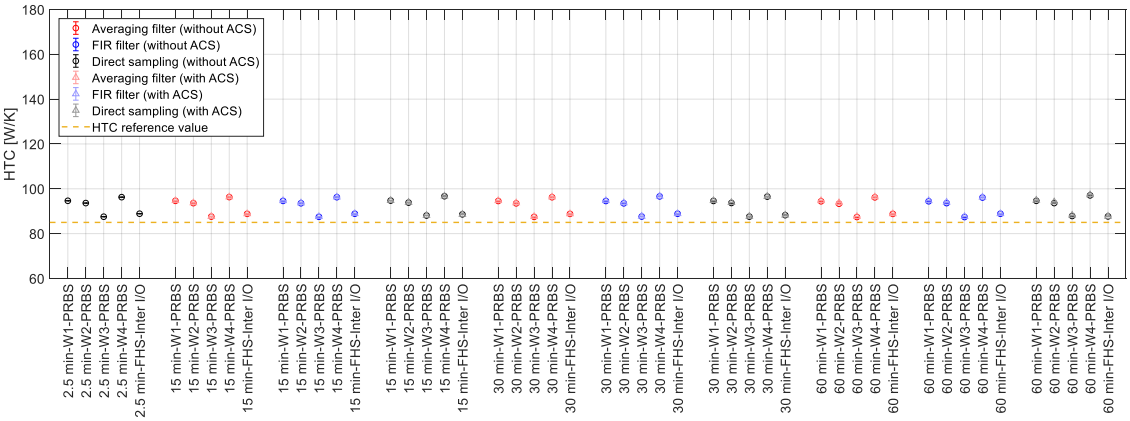

Figure 18: Identified HTC of the 1R1C deterministic model for the cases 1,2,3,4 and 14, different sampling times and pre-filtering techniques; cases with ACS are shown by triangles in lighter colors.

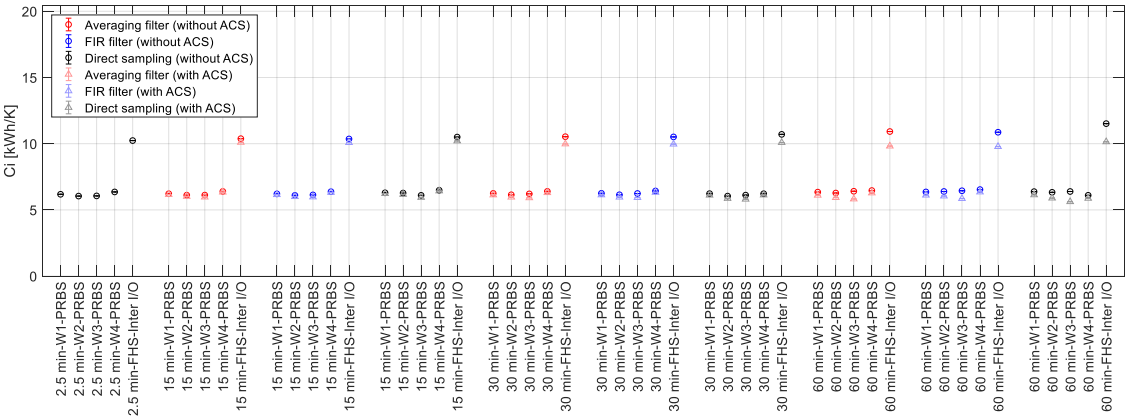

Figure 19: Identified C_i of the 1R1C deterministic model for the cases 1,2,3,4 and 14, different sampling times and pre-filtering techniques; cases with ACS are shown by triangles in lighter colors.

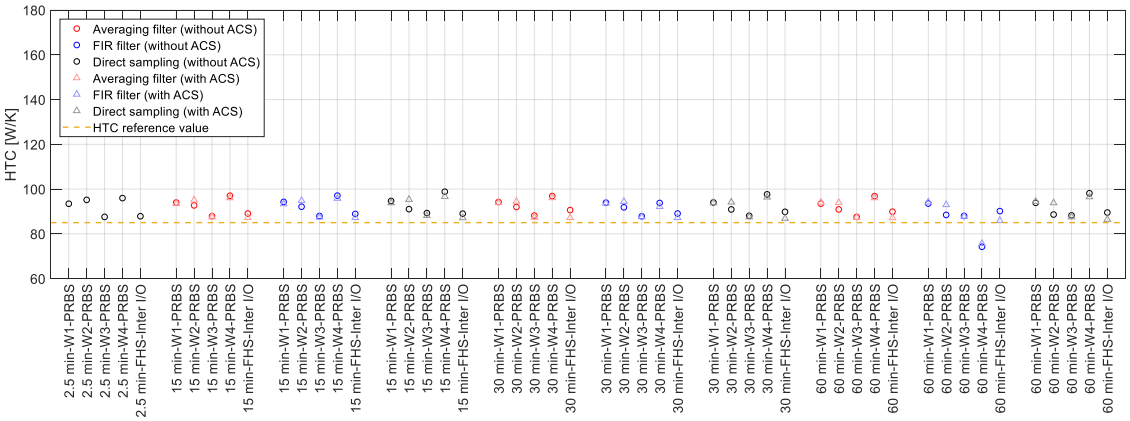

Figure 20: Identified HTC of the 1R1C stochastic model for the cases 1,2,3,4 and 14, different sampling times and pre-filtering techniques; cases with ACS are shown by triangles in lighter colors.

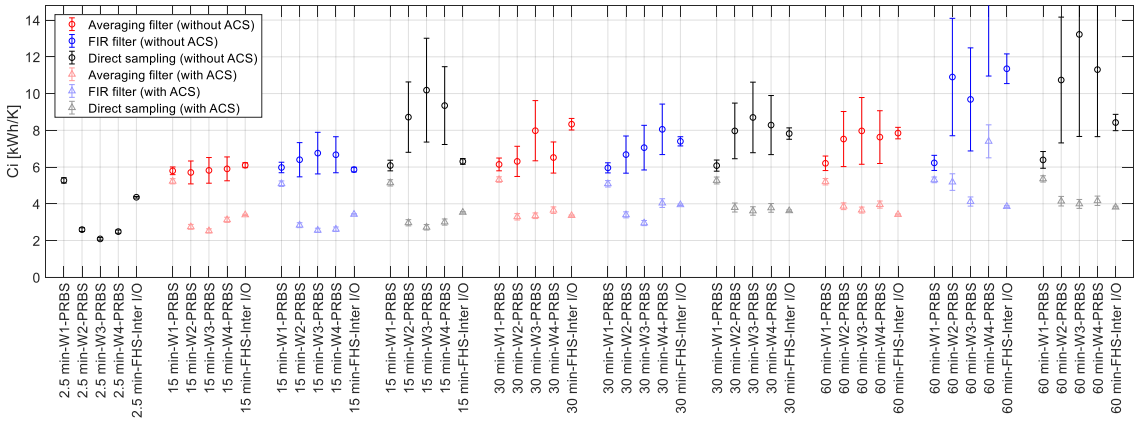

Figure 21: Identified C_i of the 1R1C stochastic model for the cases 1,2,3,4 and 14, different sampling times and pre-filtering techniques; cases with ACS are shown by triangles in lighter colors.

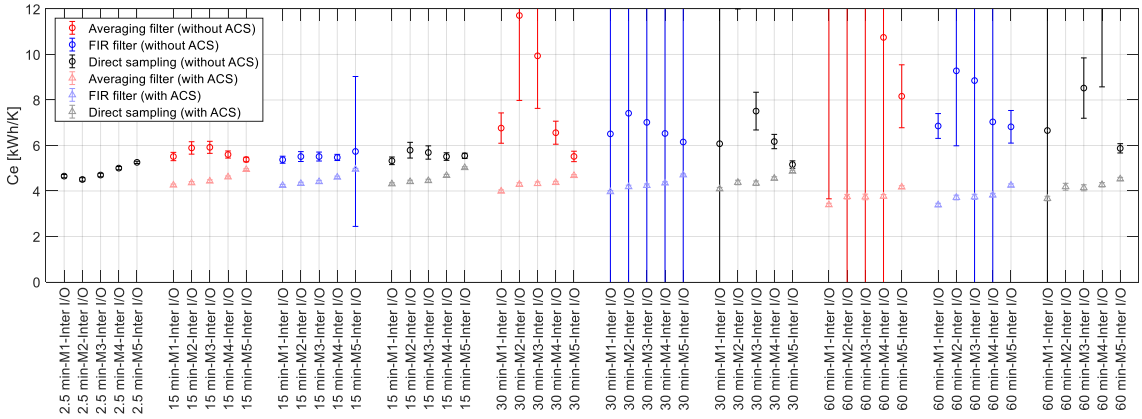

Figure 22: Identified Ce of the 3R2C stochastic model for cases 9 to 13, different sampling times and pre-filtering techniques; cases with ACS are shown by triangles in lighter colors.

References

[1] M. Hu, F. Xiao, J.B. Jørgensen, S. Wang, Frequency control of air conditioners in response to real-time dynamic electricity prices in smart grids, Appl. Energy. 242 (2019) 92–106. https://doi.org/10.1016/j.apenergy.2019.03.127.

[2] S. Stinner, K. Huchtemann, D. Müller, Quantifying the operational flexibility of building energy systems with thermal energy storages, Appl. Energy. 181 (2016) 140–154. https://doi.org/10.1016/j.apenergy.2016.08.055.

[3] G. Steindl, W. Kastner, V. Stangl, Comparison of Data-Driven Thermal Building Models for Model Predictive Control, J. Sustain. Dev. Energy, Water Environ. Syst. 7 (2019) 730–742. https://doi.org/10.13044/j.sdewes.d7.0286.

[4] P. Siano, Demand response and smart grids — A survey, Renew. Sustain. Energy Rev. 30 (2014) 461–478. https://doi.org/10.1016/j.rser.2013.10.022.

[5] A. Losi, P. Mancarella, A. Vicino, Integration of demand response into the electricity chain: challenges, opportunities, and Smart Grid solutions, John Wiley & Sons, 2015.

[6] E. Georges, B. Cornélusse, D. Ernst, V. Lemort, S. Mathieu, Residential heat pump as flexible load for direct control service with parametrized duration and rebound effect, Appl. Energy. 187 (2017) 140–153. https://doi.org/10.1016/j.apenergy.2016.11.012.

[7] J. Hu, H. Morais, T. Sousa, M. Lind, Electric vehicle fleet management in smart grids: A review of services, optimization and control aspects, Renew. Sustain. Energy Rev. 56

(2016) 1207–1226. https://doi.org/10.1016/j.rser.2015.12.014.

[8] L. Pérez-Lombard, J. Ortiz, C. Pout, A review on buildings energy consumption information, Energy Build. 40 (2008) 394–398. https://doi.org/10.1016/j.enbuild.2007.03.007.

[9] H. Harb, N. Boyanov, L. Hernandez, R. Streblow, D. Müller, Development and validation of grey-box models for forecasting the thermal response of occupied buildings, Energy Build. 117 (2016) 199–207. https://doi.org/10.1016/j.enbuild.2016.02.021.

[10] J. Le Dréau, P. Heiselberg, Energy flexibility of residential buildings using short term heat storage in the thermal mass, Energy. 111 (2016) 991–1002. https://doi.org/10.1016/j.energy.2016.05.076.

[11] G. Reynders, Quantifying the impact of building design on the potential of structural strorage for active demand response in residential buildings, 2015. https://doi.org/10.13140/RG.2.1.3630.2805.

[12] S. Danov, J. Carbonell, J. Cipriano, J. Martí-Herrero, Approaches to evaluate building energy performance from daily consumption data considering dynamic and solar gain effects, Energy Build. 57 (2013) 110–118. https://doi.org/10.1016/j.enbuild.2012.10.050.

[13] Advanced Metering System (AMS) Status and plans for installation per Q2 2016, 2016. https://www.nve.no/energy-market-and-regulation/retail-market/smart-metering-ams/.

[14] K. Vortanz, P. Zayer, How energy providers can prepare for the rollout: Roadmap for the way into the future | Wie sich Energieversorger auf den Rollout vorbereiten können: Fahrplan für den Weg in die Zukunft, BWK- Energie-Fachmagazin. 67 (2015) 30–31.

[15] R. De Coninck, F. Magnusson, J. Åkesson, L. Helsen, Toolbox for development and validation of grey-box building models for forecasting and control, J. Build. Perform. Simul. 9 (2016) 288–303. https://doi.org/10.1080/19401493.2015.1046933.

[16] E. Atam, L. Helsen, Control-Oriented Thermal Modeling of Multizone Buildings: Methods and Issues: Intelligent Control of a Building System, IEEE Control Syst. 36 (2016) 86–111. https://doi.org/10.1109/MCS.2016.2535913.

[17] X. Pang, M. Wetter, P. Bhattacharya, P. Haves, A framework for simulation-based real-time whole building performance assessment, Build. Environ. 54 (2012) 100–108.

[18] D. Picard, J. Drgoňa, M. Kvasnica, L. Helsen, Impact of the controller model complexity on model predictive control performance for buildings, Energy Build. 152 (2017) 739–751. https://doi.org/10.1016/j.enbuild.2017.07.027.

[19] H. Wolisz, H. Harb, P. Matthes, R. Streblow, D. Müller, Dynamic simulation of thermal capacity and charging/discharging performance for sensible heat storage in building wall mass, in: Proc. Build. Simul. Conf., 2013.

[20] A.E. Ruano, E.M. Crispim, E.Z.E. Conceição, M.M.J.R. Lúcio, Prediction of building's temperature using neural networks models, Energy Build. 38 (2006) 682–694. https://doi.org/10.1016/j.enbuild.2005.09.007.

[21] A. Afram, F. Janabi-Sharifi, Review of modeling methods for HVAC systems, Appl. Therm. Eng. 67 (2014) 507–519. https://doi.org/10.1016/j.applthermaleng.2014.03.055.

[22] T.P. Bohlin, Practical Grey-box Process Identification, Springer London, 2006. https://doi.org/10.1007/1-84628-403-1.

[23] J.A. Crabb, N. Murdoch, J.M. Penman, A simplified thermal response model, Build. Serv. Eng. Res. Technol. 8 (1987) 13–19.

[24] R. De Coninck, L. Helsen, Practical implementation and evaluation of model predictive control for an office building in Brussels, Energy Build. 111 (2016) 290–298.

https://doi.org/10.1016/j.enbuild.2015.11.014.

[25] Y. Zong, G.M. Böning, R.M. Santos, S. You, J. Hu, X. Han, Challenges of implementing economic model predictive control strategy for buildings interacting with smart energy systems, Appl. Therm. Eng. 114 (2017) 1476–1486. https://doi.org/10.1016/j.applthermaleng.2016.11.141.

[26] H. Viot, A. Sempey, L. Mora, J.C. Batsale, J. Malvestio, Model predictive control of a thermally activated building system to improve energy management of an experimental building: Part I—Modeling and measurements, Energy Build. 172 (2018) 94–103. https://doi.org/10.1016/j.enbuild.2018.04.055.

[27] S.F. Fux, A. Ashouri, M.J. Benz, L. Guzzella, EKF based self-adaptive thermal model for a passive house, Energy Build. 68 (2014) 811–817. https://doi.org/10.1016/j.enbuild.2012.06.016.

[28] P. Bacher, H. Madsen, Identifying suitable models for the heat dynamics of buildings, Energy Build. 43 (2011) 1511–1522. https://doi.org/10.1016/j.enbuild.2011.02.005.

[29] E. Palomo Del Barrio, G. Lefebvre, P. Behar, N. Bailly, Using model size reduction techniques for thermal control applications in buildings, Energy Build. 33 (2000) 1–14. https://doi.org/10.1016/S0378-7788(00)00060-8.

[30] G. Reynders, J. Diriken, D. Saelens, Quality of grey-box models and identified parameters as function of the accuracy of input and observation signals, Energy Build. 82 (2014) 263–274. https://doi.org/10.1016/j.enbuild.2014.07.025.

[31] X. Yu, L. Georges, M.D. Knudsen, I. Sartori, L. Imsland, Investigation of the Model Structure for Low-Order Grey-Box Modelling of Residential Buildings, in: Proc. Build. Simul. 2019 16th Conf. IBPSA, International Building Performance Simulation Association (IBPSA), 2019. https://doi.org/10.26868/25222708.2019.211209.

[32] German Association of Engineers. Calculation of transient thermal response of rooms and buildings e modelling of rooms. 91.140.10(VDI 6007), Düsseldorf: Beuth Verlag GmbH, 2012.

[33] International Organization for Standardization. Energy performance of buildings e calculation of energy use for space heating and cooling (ISO 13790:2008), Geneva, 2008.

[34] O.M. Brastein, D.W.U. Perera, C. Pfeifer, N.O. Skeie, Parameter estimation for grey-box models of building thermal behaviour, Energy Build. 169 (2018) 58–68. https://doi.org/10.1016/j.enbuild.2018.03.057.

[35] J.F. van Impe, P.A. Vanrolleghem, D.M. Iserentant, Advanced instrumentation, data interpretation, and control of biotechnological processes, Springer Science & Business Media, 2013.

[36] L. Ljung, A. Wills, Issues in sampling and estimating continuous-time models with stochastic disturbances, Automatica. 46 (2010) 925–931. https://doi.org/10.1016/j.automatica.2010.02.011.

[37] L. Ljung, System Identification Toolbox ™ User ' s Guide, (2014).

[38] S. Norge, NS 3700: 2013 Criteria for passive houses and low energy buildings-Residential buildings, (2013).

[39] T. Johnsen, K. Taksdal, J. Clauß, X. Yu, L. Georges, Influence of thermal zoning and electric radiator control on the energy flexibility potential of Norwegian detached houses, E3S Web Conf. 111 (2019) 06030. https://doi.org/10.1051/e3sconf/201911106030.

[40] A.C. Bøeng, B. Halvorsen, B.M. Larsen, Kartlegging av oppvarmingsutstyr i husholdningene, Rapp. 2014/45. (2014). https://www.ssb.no/energi-og-industri/artikler-og-publikasjoner/kartlegging-av-oppvarmingsutstyr-i-husholdningene.

[41] S. Norge, SN/TS 3031: 2016 Energy performance of buildings, Calc. Energy Needs Energy Supply. (2016).

[42] L. Lennart, System identification: theory for the user, PTR Prentice Hall, Up. Saddle River, NJ. (1999) 1–14.

[43] N.R. Kristensen, H. Madsen, S.B. Jørgensen, Parameter estimation in stochastic grey-box models, Automatica. 40 (2004) 225–237. https://doi.org/10.1016/j.automatica.2003.10.001.

[44] M.D. Knudsen, R.E. Hedegaard, T.H. Pedersen, S. Petersen, System identification of thermal building models for demand response - A practical approach, Energy Procedia. 122 (2017) 937–942. https://doi.org/10.1016/j.egypro.2017.07.426.

[45] H. Madsen, P. Bacher, G. Bauwens, A.-H. Deconinck, G. Reynders, S. Roels, E. Himpe, G. Lethé, IEA EBC Annex 58-Reliable building energy performance characterisation based on full scale dynamic measurements. Report of subtask 3, part 2: Thermal performance characterisation using time series data-statistical guidelines, (2016). https://www.iea-ebc.org/Data/publications/EBC_Annex_58_Final_Report_ST3b.pdf.

[46] K.J. Åström, Introduction to stochastic control theory, Courier Corporation, 2012.

[47] K. Arendt, M. Jradi, M. Wetter, C.T. Veje, ModestPy: An Open-Source Python Tool for Parameter Estimation in Functional Mock-up Units, in: Proc. Am. Model. Conf. 2018, Oct. 9-10, Somb. Conf. Center, Cambridge MA, USA, 2019: pp. 121–130. https://doi.org/10.3384/ecp18154121.

[48] J. Kennedy, R. Eberhart, Particle swarm optimization, in: Proc. ICNN'95-International Conf. Neural Networks, IEEE, 1995: pp. 1942–1948.

[49] Particle Swarm Optimization Algorithm - MATLAB & Simulink - MathWorks, (n.d.). https://se.mathworks.com/help/gads/particle-swarm-optimization-algorithm.html#mw_522b9230-864b-47d1-a0db-1bf6c882d862.

[50] European Comittee for Standardization, ISO 13786:2017 - Thermal performance of building components - Dynamic thermal characteristics - Calculation methods, (2017).